THE JOURNAL OF BIOLOGICAL CHEMISTRY VOL. 286, NO. 31, pp. 27706–27717, August 5, 2011

Isotopomer Profiling of *Leishmania mexicana* Promastigotes Reveals Important Roles for Succinate Fermentation and Aspartate Uptake in Tricarboxylic Acid Cycle (TCA) Anaplerosis, Glutamate Synthesis, and Growth*[S]

Received for publication, December 20, 2010, and in revised form, May 30, 2011 Published, JBC Papers in Press, June 2, 2011, DOI 10.1074/jbc.M110.213553

Eleanor C. Saunders[‡§], William W. Ng[‡§], Jennifer M. Chambers[‡§], Milica Ng[‡§], Thomas Naderer[‡§], Jens O. Krömer[¶], Vladimir A. Likić[§], and Malcolm J. McConville[‡§1]

From the [‡]Department of Biochemistry and Molecular Biology and [§]Bio21 Institute of Molecular Science and Biotechnology, University of Melbourne, Parkville, Victoria 3010 and the [¶]Australian Institute for Bioengineering and Nanotechnology, University of Queensland, St. Lucia, Queensland 4072, Australia

Leishmania **parasites proliferate within nutritionally complex niches in their sandfly vector and mammalian hosts. However, the extent to which these parasites utilize different carbon sources remains poorly defined. In this study, we have followed the incorporation of various ^{13}C-labeled carbon sources into the intracellular and secreted metabolites of *Leishmania mexicana* promastigotes using gas chromatography-mass spectrometry and ^{13}C NMR. [U-^{13}C]Glucose was rapidly incorporated into intermediates in glycolysis, the pentose phosphate pathway, and the cytoplasmic carbohydrate reserve material, mannogen. Enzymes involved in the upper glycolytic pathway are sequestered within glycosomes, and the ATP and NAD^+ consumed by these reactions were primarily regenerated by the fermentation of phosphoenolpyruvate to succinate (glycosomal succinate fermentation). The initiating enzyme in this pathway, phosphoenolpyruvate carboxykinase, was exclusively localized to the glycosome. Although some of the glycosomal succinate was secreted, most of the C4 dicarboxylic acids generated during succinate fermentation were further catabolized in the TCA cycle. A high rate of TCA cycle anaplerosis was further suggested by measurement of [U-^{13}C]aspartate and [U-^{13}C]alanine uptake and catabolism. TCA cycle anaplerosis is apparently needed to sustain glutamate production under standard culture conditions. Specifically, inhibition of mitochondrial aconitase with sodium fluoroacetate resulted in the rapid depletion of intracellular glutamate pools and growth arrest. Addition of high concentrations of exogenous glutamate alleviated this growth arrest. These findings suggest that glycosomal and mitochondrial metabolism in *Leishmania* promastigotes is tightly coupled and that, in contrast to the situation in some other trypanosomatid parasites, the TCA cycle has crucial anabolic functions.**

Leishmania spp. are parasitic protozoa that cause a spectrum of disease in humans, ranging from self-limiting cutaneous infections to disseminating infections (mucocutaneous and visceral leishmaniasis) that can lead to severe morbidity and death (1). Approximately 12 million people are infected worldwide, resulting in more than 50,000 deaths each year (2). There are no vaccines against any of these diseases, and current drug therapies are both limited and, in many cases, are being undermined by widespread resistance (2). Although the genomes of several *Leishmania* species have now been sequenced and key aspects of metabolism intensively studied, major gaps exist in our understanding of central carbon metabolism in these divergent eukaryotes (3, 4). Given the importance of intermediary metabolism for parasite growth and protection against host microbicidal processes, detailed dissection of *Leishmania* carbon metabolism may reveal new therapeutic targets (4–6).

Leishmania develop as extracellular flagellated promastigote stages within the digestive tract of the sandfly vector. This stage is transmitted to the mammalian host when the female sandfly host takes a blood meal and is rapidly phagocytosed by neutrophils and macrophages (1). Promastigotes internalized into the phagolysosome compartment of macrophages differentiate into the obligate intracellular amastigote stage that perpetuates infection in the mammalian host. Promastigote stages are readily cultivated *in vitro* and have been the focus of most metabolic studies. Like the intensively studied insect (procyclic) stage of the related trypanosomatid, *Trypanosoma brucei* (7, 8), *Leishmania* promastigotes are thought to catabolize glucose via glycolysis, with the initial enzymes in this pathway being largely or exclusively compartmentalized in modified peroxisomes, termed glycosomes (9, 10). The glycosomal catabolism of glucose to 1,3-bisphosphoglycerate requires an investment of both ATP and NAD^+, and the rate at which these cofactors are regenerated within the closed glycosomal compartment is thought to play a key role in regulating glycolytic flux (Fig. 1) (10, 11). In *T. brucei* procyclic stages, glycosomal pools of ATP and NAD^+ can be regenerated by import of cytosolic phosphoenolpyruvate and its conversion to succinate via the enzymes PEP[2] carboxykinase, malate dehydrogenase, fumarase, and NADH-dependent fumarate reductase (Fig. 1). This pathway, referred to as glycosomal succinate fermentation,

* This work was supported by the Australian National Health and Medical Research Council.

[S] The on-line version of this article (available at http://www.jbc.org) contains supplemental Figs. S1–S4.

[1] Principal research fellow of the Australian National Health and Medical Research Council. To whom correspondence should be addressed: 30 Flemington Rd., Parkville, Victoria 3010, Australia. Tel.: 61-3-8344-2342; E-mail: malcolmm@unimelb.edu.au.

[2] The abbreviations used are: PEP, phosphoenolpyruvate; CDM, completely defined media; NaFAc, sodium fluoroacetate.

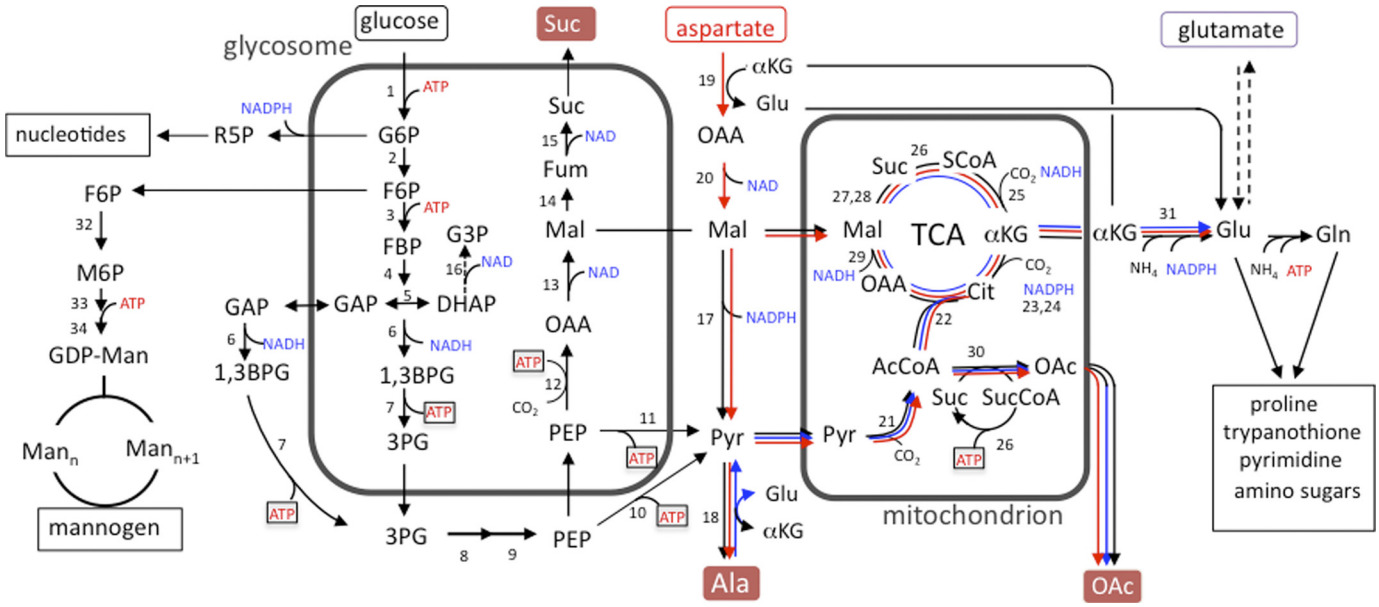

FIGURE 1. **Schematic representation of glucose, aspartate, and alanine metabolism in *Leishmania* promastigotes.** Pathways of glucose (*black lines*), aspartate (*red lines*), and alanine (*blue lines*) metabolism inferred from ^{13}C-tracer experiments in this study. The numbered reactions and their subcellular localization are supported by previous biochemical studies and genome-wide annotations (38). Note that C4 dicarboxylic acids other than malate may be exported from the glycosomes and used to replenish TCA cycle reactions in the mitochondria. Abbreviations used are as follows: *AcCoA*, acetyl-CoA; *Asp*, aspartate; *1,3BPG*, 1,3-bisphosphoglycerate; *Cit*, citrate; *FBP*, fructose-1,6-bisphosphatase; *Fum*, fumarate; *G3P*, glycerol 3-phosphate; *G6P*, glucose 6-phosphate; *Gro*, glycerol; *F6P*, fructose 6-phosphate; *M6P*, mannose 6-phosphate; *Mal*, malate; *Man$_n$*, mannogen oligomers with *n* mannose residues; *OAA*, oxaloacetic acid; *OAc*, acetate; *3PG*, 3-phosphoglycerate; *Pyr*, pyruvate; *R5P*, ribose 5-phosphate; *SCoA*, succinyl-CoA; *Suc*, succinate. Enzyme steps are as follows; *1*, hexokinase; *2*, glucose-6-phosphate isomerase; *3*, phosphofructokinase; *4*, aldolase; *5*, triose-phosphate isomerase; *6*, glyceraldehyde-3-phosphate dehydrogenase (glycosome and cytosolic isoforms); *7*, phosphoglycerate kinase (glycosome and cytosolic isoforms); *8*, phosphoglycerate mutase; *9*, enolase, *10*, pyruvate kinase; *11*, pyruvate dikinase; *12*, phosphoenolpyruvate carboxykinase (*PEPCK*); *13*, malate dehydrogenase, *14*, fumarase; *15*, NADH-dependent fumarate reductase; *16*, NADH-dependent glycerol-3-phosphate dehydrogenase; *17*, malic enzyme; *18*, alanine aminotransferase; *19*, aspartate aminotransferase; *20*, malate dehydrogenase (cytosolic isoform); *21*, pyruvate dehydrogenase complex; *22*, citrate synthase; *23*, aconitase; *24*, NADPH-dependent isocitrate dehydrogenase; *25*, α-ketoglutarate dehydrogenase; *26*, succinyl-CoA synthetase; *27*, succinate dehydrogenase; *28*, fumarase; *29*, malate dehydrogenase; *30*, acetate:succinyl-CoA-transferase; *31*, NADPH-dependent glutamate dehydrogenase; *32*, mannose-6-phosphate isomerase; *33*, mannose-6-phosphate mutase; *34*, GDP-Man pyrophosphorylase.

results in the synthesis of one ATP and two molecules of NAD^+ for each PEP imported. However, other pathways for regenerating glycosomal ATP and NAD^+ have also been identified. These include a glycerol 3-phosphate/dihydroxyacetone shuttle and reactions catalyzed by a glycerol-3-phosphate kinase, glycosomal isoforms of 3-phosphoglycerate kinase, and/or a pyruvate dikinase (10). In *T. brucei* procyclic stages, succinate fermentation appears to the major pathway for regenerating glycosomal pools of ATP/NAD^+, although other pathways may be activated if succinate fermentation is inhibited (12). *Leishmania* is thought to express a similar repertoire of enzymes for maintaining glycosomal energy/redox balance (13), although only succinate fermentation has been shown to operate *in vivo* (9, 14).

Other end products of glucose catabolism in *T. brucei* procyclic and *Leishmania* promastigotes are alanine and acetate (7, 8, 10). Alanine reflects the transamination of pyruvate, whereas acetate is primarily produced by the mitochondrial enzyme, acetate:succinyl-CoA transferase (15). Acetate:succinyl-CoA transferase participates in the metabolic cycle with succinyl-CoA synthetase to generate ATP (Fig. 1). In *T. brucei* procyclic stages, most of the acetyl-CoA synthesized in the mitochondria is hydrolyzed by acetate:succinyl-CoA transferase, and very little of the internalized glucose is oxidized in the TCA cycle (16, 17). Consistent with this conclusion, genetic deletion of *T. brucei* aconitase has no effect on procyclic metabolism (16). However, the TCA cycle of this stage is functional and is used to catabolize selected amino acids, such as proline and threonine, providing cofactors for both oxidative phosphorylation as well as substrate level phosphorylation (16, 18).

Whether a complete TCA cycle operates in *Leishmania* promastigotes is poorly defined. *Leishmania* promastigotes produce CO_2 during glucose catabolism (19) and are sensitive to respiratory chain inhibitors (*i.e.* cyanide and antimycin) (16, 20) or defects in respiratory complex proteins (21, 22), indicating that oxidative phosphorylation or other mitochondrial metabolic pathways are important for the growth of this stage. *Leishmania* promastigotes can also utilize proline when glucose-limited (5, 23), but whether proline or other amino acids are catabolized by the TCA cycle under glucose-replete conditions, as occurs in *T. brucei* procyclic stages, is unknown.

Stable isotope tracing is a powerful technique for following the metabolism of different carbon sources in microbial pathogens. Isotopic enrichment in a wide range of intracellular and secreted metabolites can be readily measured using either mass spectrometry or NMR providing quantitative information on metabolic networks (24–28). Although ^{13}C-stable isotope labeling experiments have been undertaken in *T. brucei* (29, 30), studies on *Leishmania* spp. have been limited to the use of [U-^{13}C]glucose and the detection of only a limited number of intracellular metabolites by NMR (31). In this study, we have significantly expanded this approach by using multiple ^{13}C-la-

beled carbon sources and gas chromatography-mass spectrometry (GC-MS) to increase the number and range of intracellular metabolites detected. Using this approach, we have mapped the major pathways of carbon metabolism in *Leishmania mexicana* promastigotes under glucose-replete conditions. Our results provide direct evidence for the operation of a complete TCA cycle in *Leishmania* promastigotes. Unexpectedly, we find that C4 dicarboxylic acids generated by both succinate glycosomal fermentation and the uptake and deamination of aspartate contribute to a high rate of TCA cycle anaplerosis. The replenishment of TCA cycle intermediates is needed to sustain the cataplerotic synthesis of glutamate and biosynthetically related amino acids (proline and glutamine) under physiological conditions. These findings reveal new functions for both succinate fermentation and the TCA cycle in trypanosomatid parasites. They also highlight the utility of stable isotope tracing and metabolomic approaches for identifying stage- and species-specific differences in the metabolic networks in these parasites.

EXPERIMENTAL PROCEDURES

Parasite Strains and Growth Conditions—L. mexicana wild type (WT) (MNYC/BZ/62/M379) promastigotes were cultured in M199 medium (Sigma) supplemented with 10% heat-inactivated fetal bovine serum (Invitrogen) at 27 °C. Parasites were passaged twice weekly (1:100 and 1:1000 dilutions) into fresh media to maintain log phase growth. Mid-log phase promastigotes (1×10^7 cell/ml) were harvested 2 days after inoculation of the media. Sodium fluoroacetate was used at 5 mM in growth experiments and 0.5 mM in [U-^{13}C]glucose labeling experiments.

For ^{13}C metabolic labeling experiments, log phase promastigotes were resuspended (2×10^7 cells/ml) in completely defined media (CDM) containing various ^{13}C-labeled carbon sources. CDM has the following composition: glucose (6 mM), alanine (1.9 mM), arginine (0.4 mM), glycine (3.1 mM), histidine (0.04 mM), isoleucine (0.045 mM), leucine (0.61 mM), lysine (0.55 mM), methionine (0.13 mM), phenylalanine (0.18 mM), proline (0.26 mM), serine (0.76 mM), threonine (0.34 mM), tyrosine (0.033 mM), valine (1.1 mM), and tryptophan (0.15 mM), vitamins, heme, and 0.5% bovine serum albumin (BSA) containing bound fatty acids (32). For the labeling studies, unlabeled components were replaced with the following U-^{13}C-labeled carbon sources (Cambridge Stable Isotopes): [U-^{13}C]glucose (6 mM), [U-^{13}C]alanine (1.5 mM), [U-^{13}C]aspartate (1.5 mM), [U-^{13}C]glutamine (1.5 mM), [U-^{13}C]glutamate (1.5 mM), [U-^{13}C]proline (0.26 mM), $NaH^{13}CO_3$ (1 mg/ml), or [U-^{13}C]acetate (0.12 mM). For labeling experiments with [U-^{13}C]fatty acids, a mixture of [U-^{13}C]fatty acids (Cambridge Stable Isotopes) was bound to delipidated bovine serum albumin (BSA, 1:1 molar ratio), filter-sterilized, and added to CDM at 0.5–2% (w/v).

Sampling and Metabolite Extraction—Parasite metabolism was quenched using the protocol described previously (33). Briefly, aliquots of promastigote culture medium (containing 12×10^7 parasites) were transferred to 15-ml tubes and rapidly chilled in a dry ice/ethanol slurry (~10 s to cool the cell suspension to 0 °C). The tubes were transferred to an ice bath, just before the suspension reached 0 °C (to prevent freezing), and the chilled parasites were harvested by centrifugation (805 × *g*, 10 min, 0 °C). The culture supernatant was stored at −70 °C for NMR analysis, and the cell pellet was suspended in ice-cold PBS (3 ml, 0 °C), and 4×10^7 cell eq (three replicates) were washed twice with cold PBS (10,000 × *g*, 1 min at 0 °C) and immediately extracted in chloroform/methanol/water (1:3:1 v/v, 250 μl) containing 1 nmol of *scyllo*-inositol as an internal standard. The extracts were vortex-mixed and then incubated at 60 °C for 15 min. Insoluble material was removed by centrifugation (16,100 × *g*, 0 °C, 5 min), and the supernatant was adjusted to chloroform/methanol/water (1:3:3 v/v) by addition of H_2O, vortex-mixed, and centrifuged (16,000 × *g*, 5 min) to induce phase separation. The lower phase was retained for lipid analysis, and the upper phase was transferred to a fresh microcentrifuge tube (1.5 ml) for analysis of polar metabolites.

Analysis of Polar and Apolar Metabolites by GC-MS—Polar phases were dried *in vacuo* (55 °C) in 250-μl glass GC vial inserts, and free aldehyde groups were protected by derivatization in methoxyamine hydrochloride (Sigma, 20 μl, 20 mg/ml in pyridine) with continuous mixing (25 °C, 14 h) (33). Metabolites were subsequently derivatized with *N,O*-bis(trimethylsilyl)trifluoroacetamide reagent (containing 1% trimethylchlorosilane (Pierce, 20 μl) for 1 h at 25 °C. Samples were analyzed by GC-MS using a DB5 capillary column (J&W Scientific, 30 m, 250 μm inner diameter, 0.25-μm film thickness), with a 10-m inert duraguard. The injector insert and GC-MS transfer line temperatures were 270 and 250 °C, respectively. The oven temperature gradient was programmed as follows: 70 °C (1 min); 70 °C to 295 °C at 12.5 °C/min; 295 °C to 320 °C at 25 °C/min; 320 °C for 2 min. The major carbohydrate reserve material of promastigotes, mannogen, was extracted and subjected to solvolysis in anhydrous methanolic HCl (50 μl, 0.5 M HCl, 16 h, 80 °C), and the *N,O*-bis(trimethylsilyl)trifluoroacetamide derivative of mannose methyl esters was determined by GC-MS (34). Metabolites were identified based on GC retention time and mass spectra as compared with authentic standards. The level of labeling was estimated as the percent of the metabolite pool containing one or more ^{13}C atoms. The mass isotopomer distributions of individual metabolites were corrected for the occurrence of natural isotopes of carbon, nitrogen, hydrogen, oxygen, and silicon in both the metabolite and derivatizing agent as described previously (35).

Analysis of Carbon Source Utilization and Overflow Metabolites by ^{13}C NMR—Culture supernatants (540 μl) were gently premixed with 5 mM D6-DSS in D_2O (60 μl, containing 0.2% w/v NaN_3), 21.4 mM [U-^{13}C]glycerol in D_2O (5 μl, containing 0.2% w/v NaN_3), and 21.4 mM imidazole in D_2O (5 μl, containing 0.2% w/v NaN_3), prior to analysis by NMR. ^{13}C spectra at 200 MHz were obtained using an 800 MHz Bruker-Biospin Avance fitted with a cryoprobe. Samples were maintained at 25 °C and spun at 20 Hz during sample collection. ^{13}C spectra were acquired using the Avance zgpg pulse program with power-gated ^{1}H decoupling. A pre-scan delay of 80.78 μs, a delay between pulses of 2.0 s, and an acquisition time of 0.78 s were used. For each sample, four dummy scans were followed by 4000 scans with a receiver gain set at 2050. The resulting ^{13}C

free induction decays were processed with Bruker TOPSPIN 2.0 (the exponential function with line broadening = 5.0 Hz was applied in the frequency domain prior to Fourier transform, base-line correction, and integration). Quantification was performed as published previously (36), and spectra were assigned by reference to authentic standards.

Expression of GFP-tagged PEP Carboxykinase in Promastigotes—The open reading frame of PEP carboxykinase (LmjF27.1810) was amplified by PCR using primers CTAGCGGCCGCggagctggtgcaggcgctggagccggtgccatggccccgatcatccaccg and GCTGGATCCctacagatgagccgtctccac and cloned into the NotI/BamHI sites of pXG GFP2+. For the deletion of the C-terminal tripeptide AHL, the reverse primer GCTGGATCCctacgtctccacgtacttcggcac was used instead. Clones were verified by diagnostic digests and sequencing of the entire open reading frame. Promastigotes were subsequently transfected with purified plasmids by electroporation and selected with G418 (50 μg/ml) (6). GFP-expressing parasites were immobilized onto poly-L-lysine-coated coverslips and visualized by fluorescence microscopy (Zeiss Axioplan 2 microscope). Images were compiled in Photoshop (6).

RESULTS

Carbon Source Utilization under Glucose-replete Conditions—Previous studies have shown that rapidly dividing *Leishmania* promastigotes utilize glucose as the preferred carbon source. However, the extent to which other carbon sources are co-utilized remains poorly defined. The uptake and catabolism of [U-^{13}C]glucose and other U-^{13}C-labeled carbon sources in CDM were therefore measured. As expected, rapidly dividing promastigotes preferentially utilized [U-^{13}C]glucose (Fig. 2*A*), which was catabolized to CO_2 (detected as $H^{13}CO_3^-$ by ^{13}C NMR) and the partially oxidized end products succinate, acetate, and alanine (Fig. 2*B*). A low level of [^{13}C]glutamate secretion was also observed. These results are consistent with the operation of the succinate fermentation pathway, the conversion of acetyl-CoA to acetate (via the mitochondrial acetate:succinyl-CoA transferase) and substantial flux of glycolytic end products into the TCA cycle (Fig. 1).

Unexpectedly, promastigotes also utilized significant amounts of aspartate and alanine under glucose-replete conditions (Fig. 2*A*). Both amino acids were partially catabolized to CO_2 and/or converted to succinate or acetate (Fig. 2*B*). Some of the internalized aspartate was also secreted as alanine, possibly indicating interconversion of malate and pyruvate via the malic enzyme (Fig. 2*B*). Surprisingly, neither glutamate, glutamine, nor proline were significantly internalized when these amino acids were present in the medium at 300 μM (data not shown). However, a low level of uptake of glutamate and to a lesser extent glutamine was observed when these amino acids were provided at 1.5 mM (Fig. 2, *A* and *B*). These data suggest that promastigote glutamate uptake is minimal under standard *in vitro* cultivation conditions. The uptake of aspartate/alanine appears to be important for normal growth, as promastigote proliferation in medium lacking nonessential amino acids was significantly reduced compared with growth in CDM (supplemental Fig. S1). Promastigotes internalized a range of other essential and nonessential amino acids (supplemental Fig. S2).

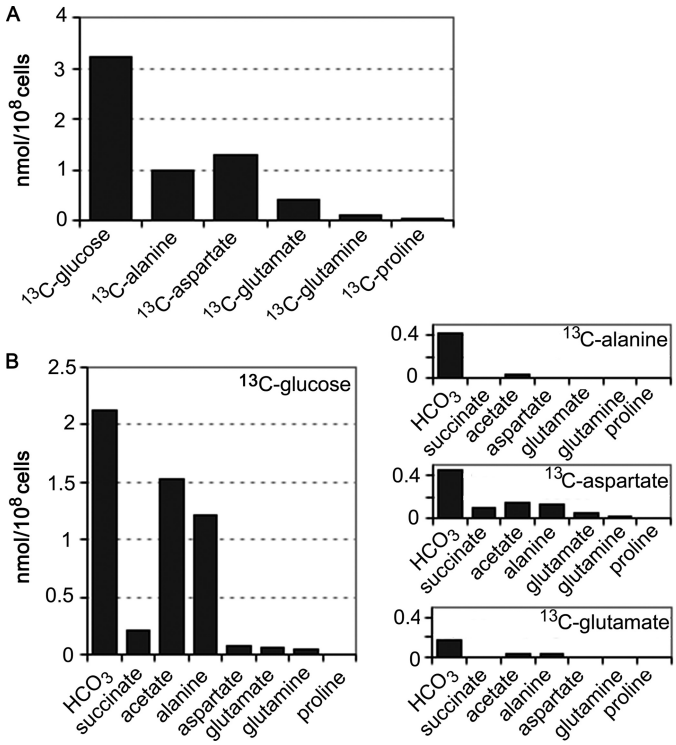

FIGURE 2. **Carbon source utilization by *L. mexicana* promastigotes.** *A*, *L. mexicana* promastigotes were cultivated in compositionally equivalent CDM containing either [U-^{13}C]glucose, [U-^{13}C]alanine, [U-^{13}C]aspartate, [U-^{13}C]glutamate, [^{13}C]glutamine, or [U-^{13}C]proline, in place of the corresponding unlabeled carbon source. The rate of uptake of different ^{13}C-labeled carbon sources was assessed by ^{13}C NMR analysis of the medium after 24 h of incubation. *B*, promastigotes were cultivated in compositionally equivalent CDM containing [U-^{13}C]glucose, [U-^{13}C]alanine, [U-^{13}C]aspartate, or [U-^{13}C]glutamate, and the major secreted end products in the medium were quantitated by ^{13}C NMR analysis after 24 h of incubation. The major secreted metabolites were carbon dioxide (detected as production of $H^{13}CO_3$), succinate, acetate, alanine, aspartate, glutamate, and glutamine (listed *below* each box).

However, none of these amino acids were actively catabolized to CO_2 or other detectable end products under these conditions. Similarly, promastigotes exhibited minimal uptake and utilization of alternative carbon sources, such as [U-^{13}C]acetate or [U-^{13}C]fatty acids (Fig. 3*B*).

Delineation of Pathways of Glucose Catabolism in L. mexicana Promastigotes—Current models of glucose catabolism in *Leishmania* have been largely inferred from analysis of secreted end products. To more precisely define the metabolic fate of glucose, the labeling of intracellular metabolite pools with [U-^{13}C]glucose was monitored using GC-MS. This method can be used to detect more than 120 metabolites in promastigote extracts, of which 30 were found to be labeled with one or more of the proffered ^{13}C-labeled carbon sources. Label derived from [U-^{13}C]glucose was rapidly incorporated into intermediates in glycolysis, the pentose phosphate pathway, glycosomal succinate fermentation, and the TCA cycle (Fig. 3, *A* and *B*). The labeling of intermediates in the glycolytic and succinate fermentation pathway/TCA cycle generally plateaued after 3 h, although a further gradual increase in enrichment occurred over 24 h (Fig. 3*A*), most likely reflecting the time needed to reach isotopic equilibration with the intracellular carbohydrate reserve, mannogen (see below), and extracellular pools of ala-

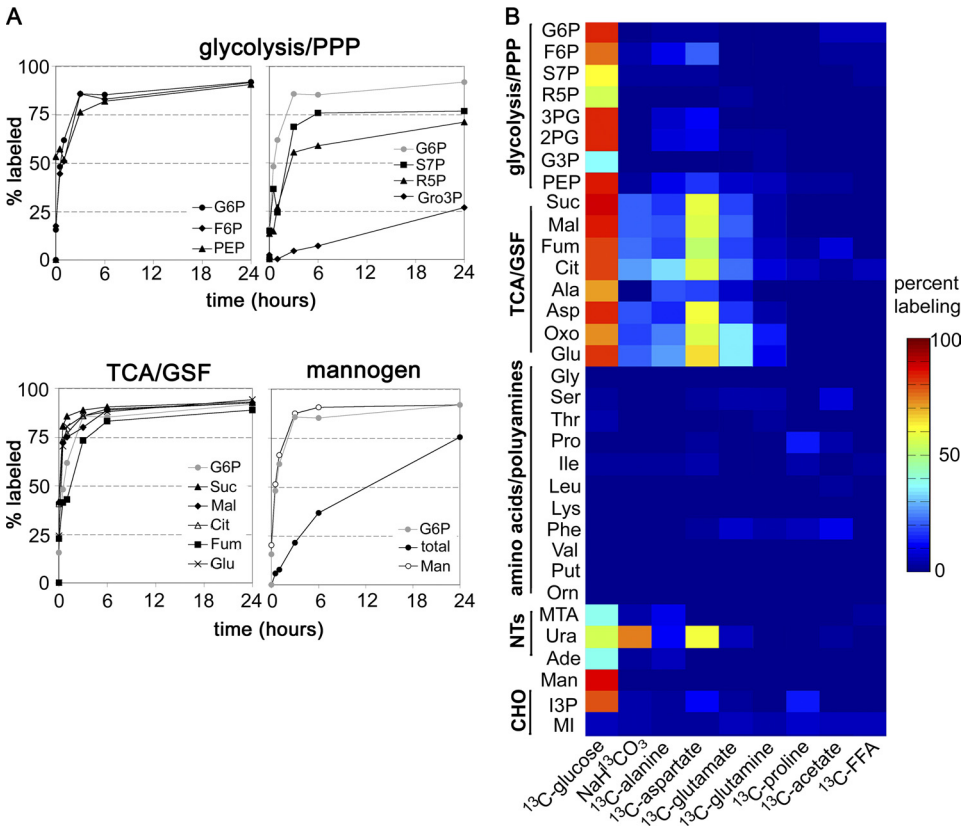

FIGURE 3. **Isotopic enrichment in intracellular metabolite pools following cultivation with different ^{13}C-labeled carbon sources.** *A, L. mexicana* promastigotes were cultivated in CDM containing [U-^{13}C]glucose, and parasites were metabolically quenched at indicated time points. Isotopic enrichment in key intracellular intermediates was determined by GC-MS (percent labeling indicates mole percent of intracellular pool labeled with one or more ^{13}C atoms after correction for natural isotopic abundance). Kinetics of labeling of selected intermediates in glycolysis (*G6P, F6P*, and *PEP*), the pentose phosphate pathway (*PPP*) (*S7P* and *R5P*), glycerol metabolism (*Gro3P*), succinate fermentation and the TCA cycle (*Suc, Mal, Cit, Fum,* and *Glu*) and the synthesis of small mannogen oligomers (*Man*) or the total mannogen pool (*total*) are shown. *B, L. mexicana* promastigotes were cultivated in compositionally equivalent CDM containing the indicated ^{13}C-labeled carbon source in place of the equivalent unlabeled nutrient. Parasites were metabolically quenched after 3 h of incubation and isotopic enrichments in 33 intermediates in central carbon metabolism determined by GC-MS and represented in the *heat map*. Abbreviations used are as follows: refer to Fig. 1 and *MTA*, 5-methylthioadenosine; *Ura*, uracil; *Ade*, adenine; *Gro3P*, glycerol 3-phosphate; *MIP*, inositol-3-phosphate; *MI*, myo-inositol; *Man$_n$*, mannogen oligomers; *S7P*, sedoheptulose-7-phosphate; *^{13}C-FFA*, mixture of ^{13}C-U-fatty acids bound to bovine serum albumin.

nine, which is both secreted and internalized (Fig. 1). The pentose phosphate pathway intermediates, ribose-5-phosphate and sedoheptulose-7-P, were labeled with slower kinetics than the glycolytic intermediates indicating a reduced flux into this pathway. However, the pentose phosphate pathway is likely to be critical for the *de novo* synthesis of nucleotides needed to maintain NTP levels and RNA/DNA synthesis, as shown by the rapid labeling of the ribose sugar moiety in the purine nucleotides, adenosine and 5-methylthioadenosine (reflecting the utilization of ATP in polyamine biosynthesis), as well as the labeling of the pyrimidine nucleoside base, uracil, in [U-^{13}C] glucose-fed parasites (Fig. 3*B* and supplemental Fig. S3).

[U-^{13}C]Glucose was also incorporated into the major carbohydrate reserve material, mannogen (Fig. 3, *A* and *B*). Mannogen is composed of short chains of β1–2-linked mannose (degree of polymerization 4–40 residues) and is exclusively located in the cytosol (34, 37). Short chain mannogen oligomers detected by GC-MS were labeled with similar kinetics to glycolytic intermediates (Fig. 3*A*) suggesting that excess glucose/fructose 6-phosphate, generated in the glycosome, is exported to the cytoplasm and converted to mannose 6-phosphate and GDP-Man (Fig. 1). Interestingly, incorporation of label into the total mannogen pool increased more slowly and had not reached equilibrium after 24 h (Fig. 2), possibly indicating the presence of a subpopulation of long chain mannogen oligomers that have a slower turnover.

Although secreted succinate accounted for less than 10% of the total glucose consumed by dividing promastigotes (Fig. 2), the rapid labeling of C4 dicarboxylic acids, malate, fumarate, and succinate, suggested that succinate fermentation plays a major role in maintaining the ATP/ADP and NAD^+/NADH balance in the glycosomes (Fig. 3*A*). This possibility was supported by isotopomer analysis of C4 dicarboxylic acids in [U-^{13}C]glucose-fed promastigotes. The major isotopomer of all three dicarboxylic acids contained three labeled carbons (+3), reflecting their synthesis from uniformly labeled PEP and incorporation of unlabeled carbonate (Fig. 4, *A* and *B*). Similarly, addition of $NaH^{13}CO_3$ to the medium led to the incorporation of a single labeled carbon into malate, fumarate, and succinate (Fig. 3*B*).

Succinate fermentation is initiated by the enzyme PEP carboxykinase, which contains a canonical glycosome-targeting motif and is predicted to be primarily localized to the glycosome from subcellular fractionation studies (38). The localization of this enzyme was confirmed by transfecting *L. mexicana* promastigotes with a plasmid encoding full-length or truncated

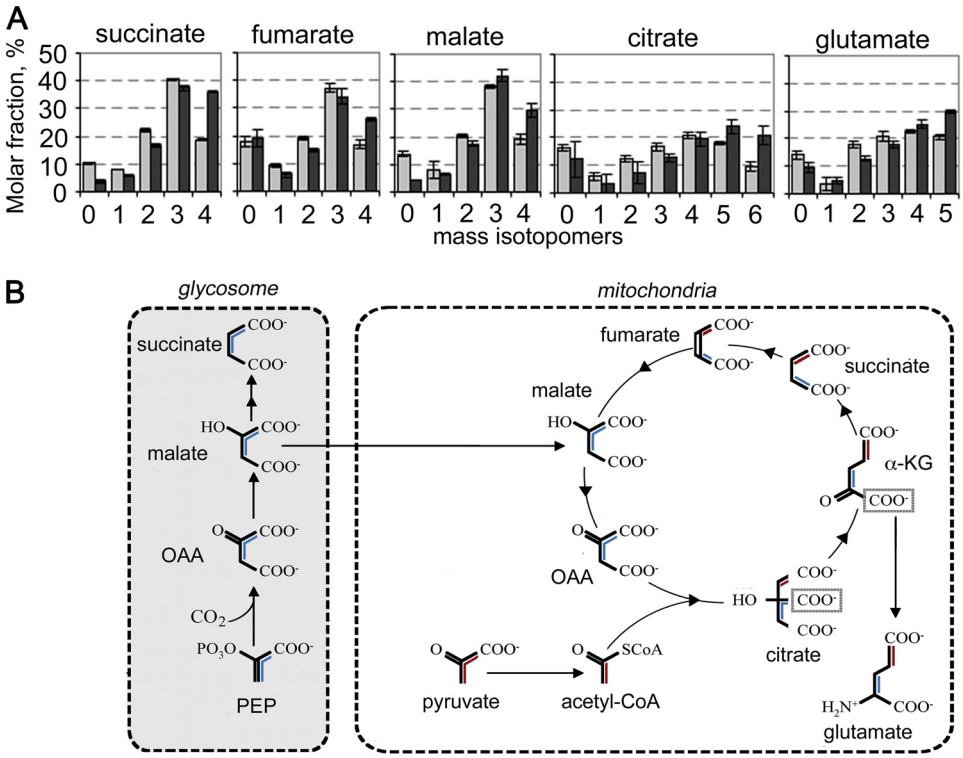

FIGURE 4. **Isotopomer analysis of key succinate fermentation/TCA cycle intermediates in [U-^{13}C]glucose-fed promastigotes.** *A*, *L. mexicana* promastigotes were cultivated in CDM containing [U-^{13}C]glucose and harvested at 3 h (*gray bar*) and 24 h (*black bar*). The relative abundance (mole percent) of the mass isotopomers (M_0, M_1, M_2, etc. containing 0, 1, 2, etc. of labeled carbons) of key intermediates in succinate fermentation and the TCA cycle were determined following correction for natural isotopic abundance (*error bars*, S.E., $n = 3$). *B*, metabolic scheme showing expected labeling of glycosomal C4 dicarboxylic acids and TCA cycle intermediates with fully labeled PEP (*blue*) or pyruvate (*red*).

PEP carboxykinase fused to GFP. As shown in Fig. 5, the fusion protein containing full-length PEP carboxykinase was exclusively targeted to punctate organelles that are indistinguishable from glycosomes (39). In contrast, the truncated fusion protein, lacking the canonical C-terminal tripeptide glycosomal targeting signal, was primarily localized in the cytosol (Fig. 5). These data suggest that succinate fermentation is initiated exclusively in the glycosomes, consistent with the proposed function of this pathway in maintaining ATP/NAD$^+$ levels in this organelle.

Studies in other trypanosomatid parasites have shown that glycosomal pools of NAD$^+$ and ATP can also be regenerated by a dihydroxyacetone/glycerol 3-phosphate shuttle, in which glycosomal dihydroxyacetone is reduced to glycerol 3-phosphate by a glycosomal NADH-dependent glycerol-3-phosphate dehydrogenase and then regenerated by a mitochondrial FAD-dependent glycerol-3-P dehydrogenase (13). The glycerol 3-phosphate produced by the glycosomal dehydrogenase can also be converted to glycerol by a glycosomal glycerol-3-P kinase to produce ATP. Although the *Leishmania* genomes encode both glycosomal enzymes needed for glycerol 3-phosphate and glycerol production (13), the flux through these pathways appears to be negligible as glycerol 3-phosphate was labeled with very slow kinetics in [U-^{13}C]glucose-fed promastigotes (Fig. 3, *A* and *B*), and glycerol was not detected in either parasite extracts or as a secreted product in the medium (data not shown). Collectively, these findings indicate that glycosomal succinate fermentation is the primary or sole pathway used to regenerate ATP and NAD$^+$ consumed during glycolysis.

Operation of a Complete TCA Cycle in Leishmania Promastigotes—A major fraction of the internalized glucose is catabolized to CO_2 indicating that most of the end products of glycolysis are further catabolized in the mitochondria (Fig. 2). The operation of a complete TCA cycle was supported by the identification of fully labeled citrate, glutamate (derived from α-ketoglutarate), fumarate, malate, and succinate (Fig. 4*A*). Uniform labeling of these intermediates indicates participation in at least two turns of the TCA cycle. Interestingly, a major fraction of intracellular citrate and glutamate (reflecting labeling of TCA cycle α-ketoglutarate) contained three labeled carbon atoms (Fig. 4*A*). The predominance of these isotopomers indicated that C4 dicarboxylic acids generated by the succinate fermentation pathway are used to replenish the TCA cycle (Fig. 4*B*). Similarly, the presence of +5-labeled citrate likely reflects synthesis from +3-labeled oxaloacetate and +2-labeled acetyl-CoA (Fig. 4, *A* and *B*). TCA cycle anaplerosis, utilizing glycosomal C4 dicarboxylic acids, was further supported by the equivalent labeling of citrate and glutamate with H^{13}CO$_3$ compared with malate, fumarate, and succinate (Fig. 3*B*). These anaplerotic processes must be matched by cataplerotic reactions, such as export of citrate for fatty acid biosynthesis or α-ketoglutarate for glutamate synthesis. Although promastigote fatty acids are labeled with [U-^{13}C]glucose (data not shown), incorporation is likely to occur via acetate produced by acetate:succinyl-CoA transferase rather than by citrate lyase (40). Conversely, the large intracellular pool of glutamate was rapidly labeled in [U-^{13}C]glucose-fed parasites (Fig. 3, *A* and *B*).

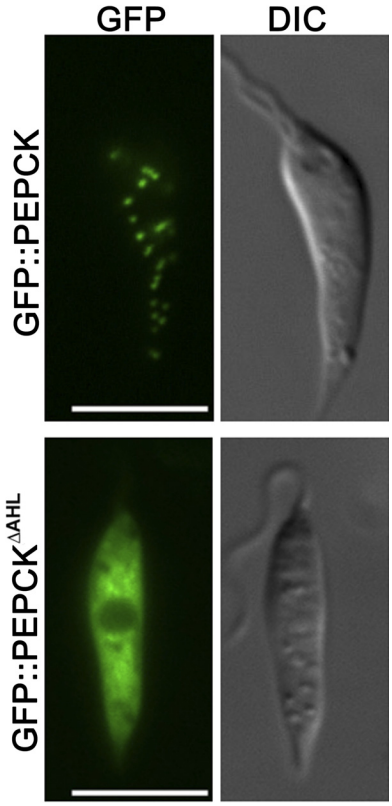

FIGURE 5. **Localization of PEP carboxykinase (PEPCK) to glycosomes.** Full-length and truncated PEP carboxykinase were expressed as GFP fusion proteins in promastigotes, and localization was determined by fluorescence microscopy. *Top,* full-length GFP::PEP carboxykinase chimera. *Bottom,* GFP::PEP carboxykinase chimera lacking the C-terminal tripeptide AHL (GFP::PEPCK$^{\Delta AHL}$). Parasites were visualized by fluorescence and differential interference contrast (*DIC*) microscopy. *Scale bar,* 5 μm.

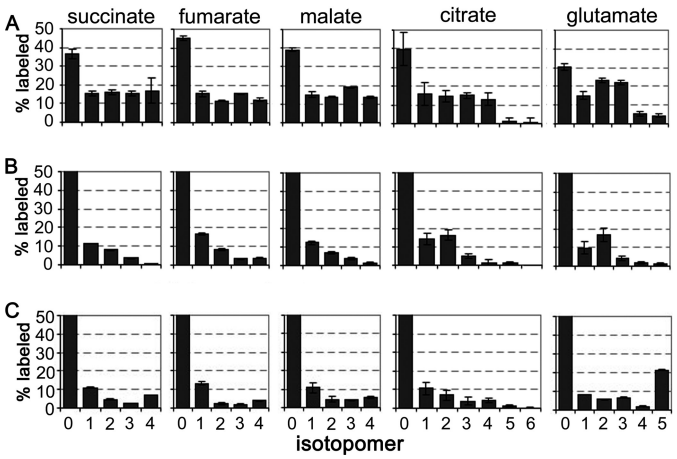

FIGURE 6. **Isotopomer analysis of central carbon metabolites in [U-^{13}C]aspartate, [U-^{13}C]alanine, and [U-^{13}C]glutamate-fed parasites.** *L. mexicana* promastigotes were cultivated in CDM containing either 1.5 mM [U-^{13}C]aspartate (*A*), 1.9 mM [U-^{13}C]alanine (*B*), or 1.5 mM [U-^{13}C]glutamate (*C*) for 3 h, and the mass isotopomers (M_0, M_1, M_2, etc. containing 0, 1, 2, etc. labeled carbons) of key intermediates in succinate fermentation and the TCA cycle quantitated by GC-MS (*error bars,* S.E., $n = 3$).

Together with the finding that promastigotes have a limited capacity to internalize glutamate or other amino acids that could be catabolized to glutamate (Fig. 2), it is likely that removal of α-ketoglutarate for glutamate synthesis is the major cataplerotic process under these growth conditions (Fig. 1).

Catabolism of Alanine, Aspartate, and Glutamate under Glucose-replete Conditions—We hypothesized that aspartate uptake under glucose-replete conditions contributes to the replenishment of TCA intermediates as well as the synthesis of glutamate via transamination reactions. This conclusion was supported by the prominent labeling of TCA cycle intermediates with [U-^{13}C]aspartate (Fig. 3) and isotopomer analysis of individual metabolite species (Fig. 6*A*). In particular, the presence of +4-labeled citrate and +3-labeled glutamate in [U-^{13}C]aspartate-labeled parasites (Fig. 6*A*) indicated that the carbon backbone of aspartate was directly incorporated into the TCA cycle. The low abundance of +5- and +6-labeled citrate or +4- and +5-labeled glutamate (Fig. 6*A*) indicated that the carbon skeleton of aspartate primarily enters the TCA cycle intact (Fig. 6*A*).

[U-^{13}C]Alanine was also internalized and catabolized in the TCA cycle (Fig. 6*B*). Labeled TCA cycle intermediates contained predominantly one or two labeled carbons, demonstrating that the internalized [U-^{13}C]alanine is deaminated to pyruvate and enters the TCA cycle via acetyl-CoA. In contrast, very little of the internalized [U-^{13}C]glutamate was catabolized in the TCA cycle, as indicated by the predominance of +5-labeled species (Fig. 6*C*). These experiments suggest that the promastigote TCA cycle has an important anabolic function in glutamate, glutamine, and proline synthesis and that internalized glutamate is primary used for biosynthetic purposes rather than being catabolized.

TCA Cycle Activity Is Required for Growth of L. mexicana Promastigotes—To investigate whether the TCA cycle is required for parasite growth, *L. mexicana* promastigotes were cultivated in the presence of the metabolic inhibitor sodium fluoroacetate (NaFAc). Incubation with NaFAc leads to the formation of fluorocitrate, a potent inhibitor of aconitase. NaFAc treatment resulted in growth arrest, although parasites remained viable over several days (Fig. 7*A*). Growth arrest occurred in the presence of 0.3 mM exogenous glutamate but was completely reversed by supplementation of the medium with 10-fold higher concentrations of glutamate (3 mM) (Fig. 8*A*). These results indicate that the operation of TCA cycle is essential for growth and that the conversion of citrate to α-ketoglutarate might be required for synthesis of glutamate under standard culture conditions.

To confirm that NaFAc is selective for the aconitase reaction, changes in key metabolite levels were determined by GC-MS at various times after addition of the inhibitor. Addition of NaFAc led to a >20-fold increase in the intracellular concentration of citrate and a pronounced increase in citrate secretion (Fig. 7, *B* and *C*). This was associated with concomitant decrease in glutamate levels, despite the presence of 0.3 mM exogenous glutamate (Fig. 7*B*). These data confirm that NaFAc specifically inhibits the aconitase reaction and biosynthesis of α-ketoglutarate/glutamate and demonstrates that glutamate uptake is insufficient to maintain cellular pools when this amino acid is present in the medium at submillimolar concentrations. Unexpectedly, NaFAc treatment had little effect on glucose uptake or the secretion of alanine and acetate (Fig. 7*D*), indicating the absence of strong feedback inhibition by citrate on glucose catabolism. Production of acetate requires a continuous supply

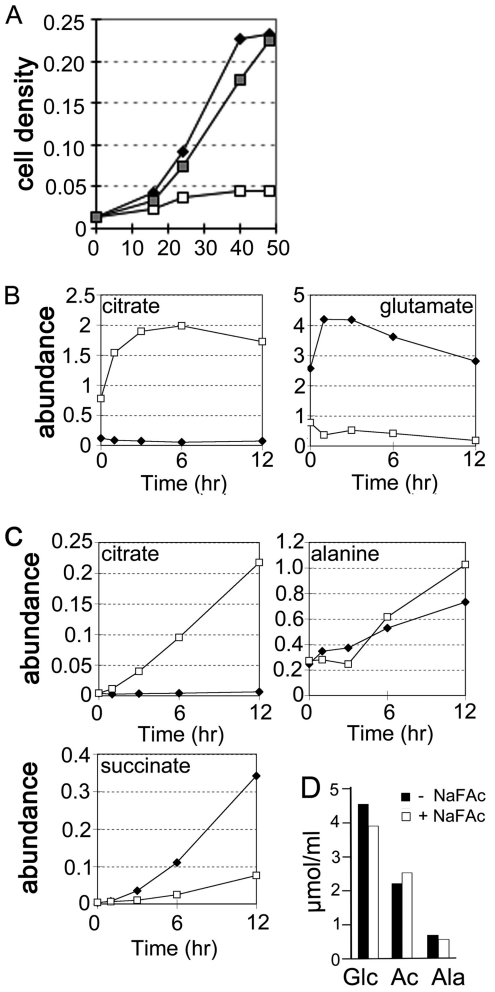

FIGURE 7. **TCA cycle is required for *L. mexicana* growth.** *A, L. mexicana* promastigotes were cultured in M199 medium containing 0.3 mM glutamate with (*open square*) or without (*closed diamond*) the aconitase inhibitor, NaFAc. Supplementation of the medium with 3 mM glutamate (*gray squares*) prevented the growth arrest induced by NaFAc. Promastigote proliferation was monitored by change in A_{600}. *B* and *C, L. mexicana* promastigotes were cultured in M199 medium, with (*open squares*) or without (*black diamonds*) 5 mM NaFAc and changes in intracellular levels of citrate and glutamate (*B*) or the secreted metabolites, citrate, alanine, and succinate (*C*) determined at the indicated time points by GC-MS. *D,* utilization of [U-^{13}C]glucose (*Glc*) and secretion of ^{13}C-labeled end products (acetate (*Ac*) and alanine (*Ala*)) by *L. mexicana* promastigotes cultivated in M199 medium in the presence (*filled bars*) or absence (*open bars*) 0.5 mM NaFAc. Values are based on ^{13}C NMR quantitation of [^{13}C]glucose, [^{13}C]acetate, and [^{13}C]alanine in the culture medium after 24 h of incubation.

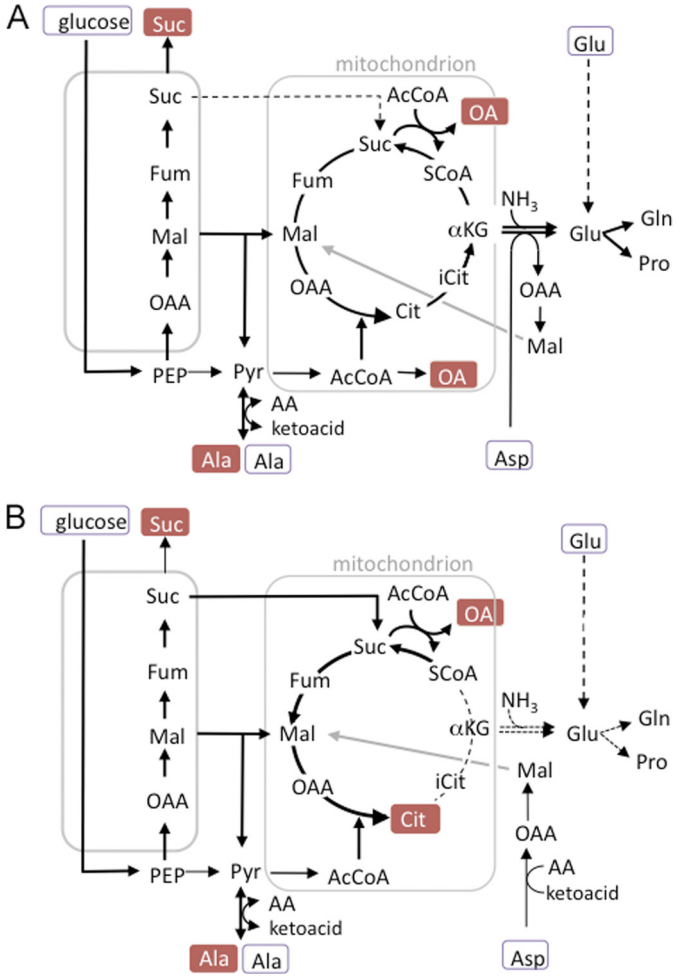

FIGURE 8. **Predicted changes in metabolic fluxes in *L. mexicana* promastigote following inhibition of the TCA cycle.** *A,* C4 dicarboxylic acids generated by succinate glycosomal fermentation and exogenous aspartate are used to replenish TCA intermediates, such as α-ketoglutarate that are removed for glutamate biosynthesis by reductive amination or transamination reactions. The glycosome contains transporters for malate, fumarate, and succinate, all of which could be transported to the mitochondria for TCA cycle anaplerosis (only transport of malate and succinate shown). Excess succinate is secreted. *B,* NaFAc treatment inhibits the mitochondrial aconitase resulting in the intracellular accumulation and secretion of citrate, with a concomitant decrease in cellular glutamate levels. Intracellular pools of glutamate can be restored by uptake of glutamate, but only when exogenous concentrations are high (*dotted line*). Other steps in the TCA cycle are maintained by the diversion of glycosomal succinate to the mitochondria and its conversion to succinyl-CoA (by acetate:succinyl-CoA transferase) or citrate. Abbreviations are as used in Fig. 1.

of succinate that is normally provided by mitochondrial succinyl-CoA synthetase (Fig. 8*A*). Following inhibition of mitochondrial aconitase, the only source of succinate would be the glycosomal pools generated by succinate fermentation. Indeed, NaFAc treatment resulted in a dramatic decrease in succinate secretion (Fig. 7*C*). Furthermore, the citrate pool in NaFAc-treated parasites contained predominantly +2-, +3-, and +5-labeled species following labeling with [U-^{13}C]glucose (supplemental Fig. S4) indicating that accumulated citrate was synthesized from glycosomal C4 dicarboxylic acids. Thus, continuous flux through the disrupted TCA cycle (from succinyl-CoA to citrate) is sustained by increased anaplerosis (Fig. 8*B*). These data suggest that operation of the TCA cycle from citrate to succinyl-CoA is critical for promastigote growth, most likely by maintaining pools of α-ketoglutarate for glutamate synthesis.

Several Pathways of Amino Acid Synthesis Are Repressed in the Presence of Exogenous Amino Acids—The *Leishmania* genomes encode all of the enzymes needed for *de novo* synthesis of serine, glycine, and proline (3, 41). They are also predicted to have most of the enzymes required for threonine biosynthesis, although gene homologues for two initiating enzymes in the canonical aspartate-phosphate pathway (aspartate kinase (EC 2.7.2.4) and β-aspartate semialdehyde dehydrogenase (EC 1.2.1.11) (supplemental Fig. S3)) have not been identified (3). The biosynthesis of these amino acids was clearly repressed in the presence of exogenous amino acids, as intracellular pools were not detectably labeled when promastigotes were labeled

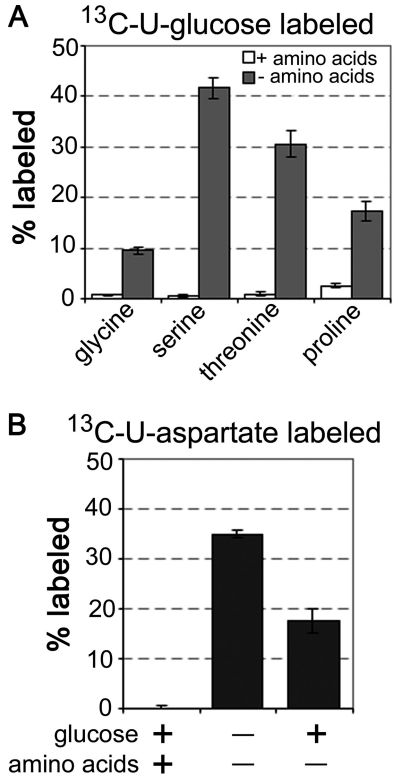

FIGURE 9. **Regulation of amino acid biosynthesis and detection of *de novo* threonine biosynthesis in *L. mexicana* promastigotes.** *A, L. mexicana* promastigotes were cultivated in CDM containing [U-^{13}C]glucose with or without amino acids for 3 h. Percent labeling of intracellular pools of glycine, serine, threonine, and proline was determined by GC-MS. *B,* promastigotes were cultivated in [U-^{13}C]aspartate-containing CDM with or without glucose or other amino acids for 3 h. Percent labeling of intracellular pool of threonine was determined by GC-MS.

with [U-^{13}C]glucose in full CDM (Fig. 3*B*). In contrast, label was incorporated into glycine, serine, proline, and threonine when promastigotes were labeled with [U-^{13}C]glucose in amino acid-deficient CDM (Fig. 9*A*). Threonine was also efficiently labeled with [U-^{13}C]aspartate, indicating synthesis via the β-aspartyl phosphate pathway. Labeling with [U-^{13}C]aspartate was increased in the absence of glucose, as expected given that glucose catabolism contributes to the formation unlabeled aspartate (Fig. 9*B*). These findings support the conclusion that key enzymes involved in amino acid biosynthesis are constitutively expressed, but are under tight allosteric control, ensuring the utilization of exogenous nutrient sources.

DISCUSSION

Genome-wide reconstructions of the *Leishmania* metabolic network have provided a broad overview of the metabolic potential of these parasites (41, 42). However, direct experimental evidence for the operation of specific pathways is limited. We have coupled ^{13}C-labeling experiments with comprehensive GC-MS metabolite profiling to investigate carbon metabolism in *L. mexicana* promastigotes under glucose-replete conditions. Our analyses suggest that there are significant differences in the way promastigote carbon metabolism is hardwired compared with other trypanosomatids. In particular, our studies reveal an expanded role for succinate fermentation and aspartate/alanine uptake in TCA cycle anaplerosis and the synthesis of glutamate. These findings are incorporated into a new model of *Leishmania* carbon metabolism outlined in Figs. 1 and 8.

Glucose, internalized by *L. mexicana* facilitative hexose transporters, is phosphorylated in the glycosome and catabolized by either the glycolytic or pentose phosphate pathways. Although the first five enzymes in the glycolytic pathway are primarily or exclusively targeted to the glycosomes, the first committed enzyme in the pentose phosphate pathway is primarily located in the cytosol (38) indicating that some of the newly formed glucose 6-phosphate is exported to the cytosol. Although pentose phosphate pathway intermediates were labeled with slower kinetics compared with glycolytic intermediates, this pathway is likely to be important for both the generation of NADPH and production of ribose 5-phosphate for nucleotide biosynthesis in rapidly dividing promastigote (as shown by the rapid labeling of several nucleotides). [U-^{13}C]Glucose was also incorporated into the major carbohydrate reserve material, mannogen. These oligosaccharides are synthesized in the cytosol,[3] requiring an additional flux of hexose 6-phosphate from the glycosomes. The rapid labeling of mannogen oligomers was unexpected as this unusual carbohydrate reserve material (including oligomers of β1–2-linked mannose) is maintained at low steady state levels in log phase parasites and only accumulates at the end of log growth and beginning of stationary growth (34). Although previous studies have shown that mannogen is rapidly mobilized under glucose starvation conditions (34), our data suggest that mannogen is also constitutively synthesized and catabolized under conditions of glucose excess. Mannogen turnover could provide a mechanism for regulating cytosolic hexose phosphate levels and fluxes through other essential metabolic pathways, such as the pentose phosphate pathway, amino sugar biosynthesis, and *N*-glycosylation (43, 44).

To sustain a high glycolytic flux in the promastigote glycosomes, as well as the export of sugar phosphates, the ATP and NAD^+ consumed in the early glycolytic reactions must be regenerated. Our data indicate that this is primarily accomplished by succinate fermentation. Although NAD^+ could also be regenerated by a glycosomally located NADH-dependent glycerol-3-phosphate dehydrogenase, flux into this pathway was very low indicating a negligible contribution to glycosomal redox balancing. The succinate fermentation pathway is initiated by PEP carboxykinase, encoded by a single copy gene. We show here that this enzyme is efficiently targeted to the glycosomes via a canonical C-terminal glycosome/peroxisome targeting signal (Fig. 5). The carboxylation of PEP results in the production of ATP, whereas subsequent steps in this pathway catalyzed by malate dehydrogenase and a NADH-dependent fumarate reductase regenerate NAD^+. Intriguingly, *L. mexicana* promastigotes express cytosolic and glycosomal isoforms of both glyceraldehyde-3-phosphate dehydrogenase (45) and 3-phosphoglycerate kinase (46, 47), which could, in principal, remove the need for succinate fermentation by relieving the need to use glycosomal pools of NAD^+ and/or providing an

[3] J. E. Ralton, M. F. Sernee, and M. J. McConville, unpublished data.

additional mechanism for synthesizing ATP, respectively. Although succinate fermentation may increase the metabolic flexibility of *Leishmania* glycosomes, it may therefore not be essential for redox/energy balancing in *Leishmania*, as has recently shown to be the case in *T. brucei* procyclic stages (12). However, as outlined below, we propose that succinate fermentation has a second and possibly more important role in TCA cycle anaplerosis in *Leishmania*.

In marked contrast to the situation in *T. brucei* procyclic stages, we show that a major fraction of the internalized glucose is fully catabolized to CO_2 in a complete TCA cycle. The operation of a complete cycle was demonstrated by the generation of uniformly labeled citrate and glutamate and production of $H^{13}CO_3^-$ in [U-^{13}C]glucose-fed promastigotes. Moreover, inhibition of the TCA cycle with sodium fluoroacetate resulted in the marked accumulation of citrate and growth arrest. A similar growth arrest can be induced by treating *L. mexicana* promastigotes with inhibitors of the respiratory chain (cyanide and antimycin) suggesting that oxidation of glucose in the TCA cycle is important for energy generation (20). However, respiratory chain inhibitors can also inhibit the operation of the TCA cycle[4] raising the possibility that growth inhibition may be a consequence of loss of TCA cycle anabolic functions, rather than decreased energy production. A major anabolic role for the TCA cycle was initially suggested by the finding that most of the C4 dicarboxylic acids generated by succinate fermentation are used to replenish TCA cycle intermediates. The recycling of glycosomal C4 acids is consistent with the observed low rate of secretion of succinate under the growth conditions used here. A high rate of TCA cycle anaplerosis was also indicated by the uptake of aspartate in glucose-rich medium and the catabolism of oxaloacetic acid carbon skeleton in the TCA cycle. Collectively, these data suggest that the promastigote TCA cycle functions as both a complete cycle (providing a source of reducing equivalents for oxidative phosphorylation as well as substrate level phosphorylation via the acetate:succinyl-CoA transferase/succinyl-CoA synthetase metabolic cycle) and as a source of biosynthetic precursors for anabolic processes that require continued replenishment of TCA cycle intermediates.

The major anabolic function of the TCA cycle is likely to be the synthesis of glutamate. Glutamate is the most abundant free amino acid in promastigote stages (data not shown) but is internalized at a low rate under standard culture conditions. Although the *Leishmania* glutamate transporter has not been identified, uptake experiments suggest that the promastigote glutamate transporter(s) have a high K_m value (48). Conversely, a high rate of *de novo* glutamate synthesis were suggested by the rapid labeling of this amino acid with [U-^{13}C]glucose, [U-^{13}C]aspartate, [U-^{13}C]alanine, and $H^{13}CO_3^-$. Most significantly, intracellular glutamate levels were rapidly depleted following inhibition of TCA cycle aconitase with NaFAc. This decrease occurred even when parasites were cultivated in the presence of 0.3 mM glutamate, indicating that glutamate uptake is not increased when *de novo* synthesis is inhibited. Glutamate is synthesized from α-ketoglutarate by glutamate dehydrogenase (38) or by transamination reactions. The *L. mexicana* glutamate dehydrogenase is located in the cytosol and, to a lesser extent, the mitochondrion (38). It utilizes NADPH, which could be provided by the pentose phosphate pathway, the malic enzyme, or the NADPH-dependent mitochondrial isocitrate dehydrogenase (49). Alternatively, *Leishmania* express a range of transaminases that are selective for specific amino acid/keto acid pairs (*i.e.* for alanine/α-ketoglutarate and aspartate/α-ketoglutarate) or have a broad specificity (50, 51). These transamination reactions are likely to be important for glutamate synthesis as *L. mexicana* promastigotes grew more slowly in medium lacking nonessential amino acids, such as aspartate and alanine, that could provide amino groups for glutamate synthesis as well as additional carbon skeletons. Interestingly, alanine was both internalized and secreted during growth on glucose. This may reflect the competing functions of the alanine aminotransferase (and potentially other amino transferases) in regulating the intracellular levels of pyruvate *versus* its role in regulating amino acid biosynthesis.

The maintenance of intracellular glutamate pools is likely to be critical for promastigote growth. Glutamate is the precursor for other amino acids, such as proline and glutamine, that are both internalized at low rates under standard culture conditions. Glutamine is also required for pyrimidine and hexosamine biosynthesis (44, 52), as well as the synthesis of the major thiols of these parasites, glutathione and trypanothione (53, 54). Trypanothione participates in many anabolic and redox processes and can be conjugated to other metabolites necessitating continuous synthesis (53, 54). Given the importance of glutamate for *Leishmania* growth and pathogenesis, it is curious why this parasite has such a limited capacity to take up this amino acid. Although the *Leishmania* glutamate transport has not been studied in detail (48), leakage of intracellular pools was clearly detected during rapid growth (Fig. 2). Limited transporter expression may therefore be essential for maintaining high intracellular concentrations and preventing release when exogenous glucose/glutamate levels are low.

Our results suggest that metabolic fluxes in the glycosome and mitochondrial are intimately linked. Isotopomer analysis indicated that the majority of the C4 dicarboxylic acids generated during glycosomal succinate fermentation are subsequently used for TCA cycle anaplerosis. Export of C4 dicarboxylic acids from glycosomes could occur via malate or succinate transporters, whereas import into the mitochondria could occur via a malate/α-ketoglutarate transporter that would ensure a balance between anaplerotic and cataplerotic fluxes across the mitochondrion membrane. This inter-organellar flux increased when the TCA cycle was inhibited with NaFAc, as shown by maintenance of acetate secretion (requiring continuous production of mitochondrial succinate) at the expense of succinate secretion. Based on these observations, we propose that succinate fermentation has two major roles in *Leishmania* as follows: to maintain the energy/redox balance of glycosomes and to replenish TCA cycle intermediates lost via cataplerotic reactions such as glutamate synthesis (Fig. 8*A*).

These findings have important implications for the biology of *Leishmania* in both the insect and mammalian hosts. Although it is commonly assumed that *Leishmania* promastigotes utilize

[4] E. C. Saunders, D. Tull, and M. J. McConville, unpublished data.

a range of carbon sources in the sandfly vector, including sugars, amino acids, and fatty acids, our data suggest that hexose availability may be a key factor regulating promastigote expansion in the mid-gut after the initial digestion of the blood meal. In contrast, amino acid levels in the mid-guts of trypanosomatid vectors are unlikely to be sufficient to sustain rapid growth (55). A dependence on carbohydrate metabolism is supported by the presence of multiple sugar kinases in the *Leishmania* genomes (3) and may reflect the abundance of sugars in the sandfly mid-gut, particularly at later stages of infection when infected female sandflies feed on plants and sugar-rich honeydews (56). Intriguingly, hexose uptake and catabolism has also been shown to be essential for the survival and proliferation of *L. mexicana* and *L. major* amastigotes in the mammalian host (6, 5) despite the fact that the macrophage phagolysosome appears to be a sugar-poor niche (39). Although the macrophage phagolysosome is expected to have relatively high levels of amino acids, amastigotes may still be limited in their capacity to salvage key amino acids such as glutamate, glutamine, and proline. Continued uptake of hexose and mitochondrial metabolism may therefore be required to maintain intracellular levels of these amino acids.

Finally, ^{13}C-tracer experiments provide a useful tool for filling gaps in predicted metabolic networks and identifying allosteric regulatory mechanisms. Specifically, most predicted pathways of amino acid biosynthesis were effectively repressed when promastigotes were cultivated in complex medium, as indicated by the absence of label in specific amino acid pools in [U-^{13}C]glucose-fed promastigotes. Pathways for the *de novo* synthesis of serine, glycine, proline, and threonine were all activated when promastigotes were suspended in amino acid-free CDM, indicating that the enzymes involved in these pathways are constitutively expressed. Significantly, previous genome-wide analyses had failed to identify enzymes required for the formation of aspartyl-β-phosphate, the first committed intermediate in threonine biosynthesis (3). The presence of a complete pathway for *de novo* synthesis of threonine was supported by complementary labeling experiments with [U-^{13}C]aspartate (Fig. 9), whereas re-examination of the *Leishmania* genomes led to the identification of candidate genes for an aspartate kinase (LmjF26.2710, a member of the aspartate/glutamate/uridylate kinase family) and an β-aspartate semialdehyde dehydrogenase (LmjF09.0390).

In summary, this study provides further insights into the diversity of carbon metabolism in trypanosomatid parasites (8). In particular, we have identified significant differences in glucose catabolism in *Leishmania* promastigotes compared with the insect stages of *T. brucei* that were not anticipated from genome analysis and existing biochemical approaches. The utilization of the comprehensive ^{13}C-tracer approach developed here will be useful for identifying new and/or unanticipated pathways in these parasites that could be exploited in the development of new drugs.

REFERENCES

1. Murray, H. W., Berman, J. D., Davies, C. R., and Saravia, N. G. (2005) *Lancet* **366,** 1561–1577
2. Croft, S. L., Sundar, S., and Fairlamb, A. H. (2006) *Clin. Microbiol. Rev.* **19,** 111–126
3. Opperdoes, F. R., and Coombs, G. H. (2007) *Trends Parasitol.* **23,** 149–158
4. Saunders, E. C., DE Souza, D. P., Naderer, T., Sernee, M. F., Ralton, J. E., Doyle, M. A., Macrae, J. I., Chambers, J. L., Heng, J., Nahid, A., Likic, V. A., and McConville, M. J. (2010) *Parasitology* **137,** 1303–1313
5. Burchmore, R. J., Rodriguez-Contreras, D., McBride, K., Merkel, P., Barrett, M. P., Modi, G., Sacks, D., and Landfear, S. M. (2003) *Proc. Natl. Acad. Sci. U.S.A.* **100,** 3901–3906
6. Naderer, T., Heng, J., and McConville, M. J. (2010) *PLoS Pathog.* **6,** e1001245
7. Bringaud, F., Rivière, L., and Coustou, V. (2006) *Mol. Biochem. Parasitol.* **149,** 1–9
8. Tielens, A. G., and van Hellemond, J. J. (2009) *Trends Parasitol.* **25,** 482–490
9. Hart, D. T., and Coombs, G. H. (1982) *Exp. Parasitol.* **54,** 397–409
10. Michels, P. A., Bringaud, F., Herman, M., and Hannaert, V. (2006) *Biochim. Biophys. Acta* **1763,** 1463–1477
11. Opperdoes, F. R. (1987) *Annu. Rev. Microbiol.* **41,** 127–151
12. Ebikeme, C., Hubert, J., Biran, M., Gouspillou, G., Morand, P., Plazolles, N., Guegan, F., Diolez, P., Franconi, J. M., Portais, J. C., and Bringaud, F. (2010) *J. Biol. Chem.* **285,** 32312–32324
13. Guerra, D. G., Decottignies, A., Bakker, B. M., and Michels, P. A. (2006) *Mol. Biochem. Parasitol.* **149,** 155–169
14. Cazzulo, J. J., Franke de Cazzulo, B. M., Engel, J. C., and Cannata, J. J. (1985) *Mol. Biochem. Parasitol.* **16,** 329–343
15. Rivière, L., van Weelden, S. W., Glass, P., Vegh, P., Coustou, V., Biran, M., van Hellemond, J. J., Bringaud, F., Tielens, A. G., and Boshart, M. (2004) *J. Biol. Chem.* **279,** 45337–45346
16. van Weelden, S. W., Fast, B., Vogt, A., van der Meer, P., Saas, J., van Hellemond, J. J., Tielens, A. G., and Boshart, M. (2003) *J. Biol. Chem.* **278,** 12854–12863
17. Coustou, V., Besteiro, S., Biran, M., Diolez, P., Bouchaud, V., Voisin, P., Michels, P. A., Canioni, P., Baltz, T., and Bringaud, F. (2003) *J. Biol. Chem.* **278,** 49625–49635
18. van Weelden, S. W., van Hellemond, J. J., Opperdoes, F. R., and Tielens, A. G. (2005) *J. Biol. Chem.* **280,** 12451–12460
19. ter Kuile, B. H. (1997) *J. Bacteriol.* **179,** 4699–4705
20. Van Hellemond, J. J., and Tielens, A. G. (1997) *Mol. Biochem. Parasitol.* **85,** 135–138
21. Uboldi, A. D., Lueder, F. B., Walsh, P., Spurck, T., McFadden, G. I., Curtis, J., Likic, V. A., Perugini, M. A., Barson, M., Lithgow, T., and Handman, E. (2006) *Int. J. Parasitol.* **36,** 1499–1514
22. Dey, R., Meneses, C., Salotra, P., Kamhawi, S., Nakhasi, H. L., and Duncan, R. (2010) *Mol. Microbiol.* **77,** 399–414
23. Mazareb, S., Fu, Z. Y., and Zilberstein, D. (1999) *Exp. Parasitol.* **91,** 341–348
24. Eylert, E., Schär, J., Mertins, S., Stoll, R., Bacher, A., Goebel, W., and Eisenreich, W. (2008) *Mol. Microbiol.* **69,** 1008–1017
25. Fan, T. W., Lane, A. N., Higashi, R. M., Farag, M. A., Gao, H., Bousamra, M., and Miller, D. M. (2009) *Mol. Cancer* **8,** 41
26. Eylert, E., Herrmann, V., Jules, M., Gillmaier, N., Lautner, M., Buchrieser, C., Eisenreich, W., and Heuner, K. (2010) *J. Biol. Chem.* **285,** 22232–22243
27. Olszewski, K. L., Mather, M. W., Morrisey, J. M., Garcia, B. A., Vaidya, A. B., Rabinowitz, J. D., and Llinás, M. (2010) *Nature* **466,** 774–778
28. Eisenreich, W., Dandekar, T., Heesemann, J., and Goebel, W. (2010) *Nat. Rev. Microbiol.* **8,** 401–412
29. Coustou, V., Biran, M., Besteiro, S., Rivière, L., Baltz, T., Franconi, J. M., and Bringaud, F. (2006) *J. Biol. Chem.* **281,** 26832–26846
30. Coustou, V., Biran, M., Breton, M., Guegan, F., Rivière, L., Plazolles, N., Nolan, D., Barrett, M. P., Franconi, J. M., and Bringaud, F. (2008) *J. Biol. Chem.* **283,** 16342–16354
31. Rainey, P. M., and MacKenzie, N. E. (1991) *Mol. Biochem. Parasitol.* **45,** 307–315
32. Merlen, T., Sereno, D., Brajon, N., Rostand, F., and Lemesre, J. L. (1999) *Am. J. Trop. Med. Hyg.* **60,** 41–50
33. De Souza, D. P., Saunders, E. C., McConville, M. J., and Likiæ, V. A. (2006) *Bioinformatics* **22,** 1391–1396
34. Ralton, J. E., Naderer, T., Piraino, H. L., Bashtannyk, T. A., Callaghan, J. M.,

and McConville, M. J. (2003) *J. Biol. Chem.* **278,** 40757–40763
35. Zamboni, N., Fendt, S. M., Rühl, M., and Sauer, U. (2009) *Nat. Protoc.* **4,** 878–892
36. Lutz, N. W., Yahi, N., Fantini, J., and Cozzone, P. J. (1996) *Magn. Reson. Med.* **36,** 788–795
37. Sernee, M. F., Ralton, J. E., Dinev, Z., Khairallah, G. N., O'Hair, R. A., Williams, S. J., and McConville, M. J. (2006) *Proc. Natl. Acad. Sci. U.S.A.* **103,** 9458–9463
38. Mottram, J. C., and Coombs, G. H. (1985) *Exp. Parasitol.* **59,** 265–274
39. Naderer, T., Ellis, M. A., Sernee, M. F., De Souza, D. P., Curtis, J., Handman, E., and McConville, M. J. (2006) *Proc. Natl. Acad. Sci. U.S.A.* **103,** 5502–5507
40. Rivière, L., Moreau, P., Allmann, S., Hahn, M., Biran, M., Plazolles, N., Franconi, J. M., Boshart, M., and Bringaud, F. (2009) *Proc. Natl. Acad. Sci. U.S.A.* **106,** 12694–12699
41. Doyle, M. A., MacRae, J. I., De Souza, D. P., Saunders, E. C., McConville, M. J., and Likiæ, V. A. (2009) *BMC Syst. Biol.* **3,** 57
42. Chavali, A. K., Whittemore, J. D., Eddy, J. A., Williams, K. T., and Papin, J. A. (2008) *Mol. Syst. Biol.* **4,** 177
43. Maugeri, D. A., Cazzulo, J. J., Burchmore, R. J., Barrett, M. P., and Ogbunude, P. O. (2003) *Mol. Biochem. Parasitol.* **130,** 117–125
44. Naderer, T., Wee, E., and McConville, M. J. (2008) *Mol. Microbiol.* **69,** 858–869
45. Hannaert, V., Blaauw, M., Kohl, L., Allert, S., Opperdoes, F. R., and Michels, P. A. (1992) *Mol. Biochem. Parasitol.* **55,** 115–126
46. McKoy, G., Badal, M., Prescott, Q., Lux, H., and Hart, D. T. (1997) *Mol. Biochem. Parasitol.* **90,** 169–181
47. Adjé, C. A., Opperdoes, F. R., and Michels, P. A. (1997) *Mol. Biochem. Parasitol.* **90,** 155–168
48. Paes, L. S., Galvez Rojas, R. L., Daliry, A., Floeter-Winter, L. M., Ramirez, M. I., and Silber, A. M. (2008) *J. Eukaryot. Microbiol.* **55,** 382–387
49. Leroux, A. E., Maugeri, D. A., Cazzulo, J. J., and Nowicki, C. (2011) *Mol. Biochem. Parasitol.* **177,** 61–64
50. Marciano, D., Maugeri, D. A., Cazzulo, J. J., and Nowicki, C. (2009) *Mol. Biochem. Parasitol.* **166,** 172–182
51. Vernal, J., Cazzulo, J. J., and Nowicki, C. (1998) *Mol. Biochem. Parasitol.* **96,** 83–92
52. Carter, N. S., Yates, P., Arendt, C. S., Boitz, J. M., and Ullman, B. (2008) *Adv. Exp. Med. Biol.* **625,** 141–154
53. Wyllie, S., Cunningham, M. L., and Fairlamb, A. H. (2004) *J. Biol. Chem.* **279,** 39925–39932
54. Dormeyer, M., Reckenfelderbäumer, N., Ludemann, H., and Krauth-Siegel, R. L. (2001) *J. Biol. Chem.* **276,** 10602–10606
55. Balogun, R. A. (1974) *Comp. Biochem. Physiol. A Comp. Physiol.* **49,** 215–222
56. Schlein, Y., and Jacobson, R. L. (1994) *Am. J. Trop. Med. Hyg.* **50,** 20–27